# Nanoscale Disorder in $CaCu_3Ti_4O_{12}$: A New Route to the Enhanced Dielectric Response

Y. Zhu,[1,*] J. C. Zheng,[1] L. Wu,[1] A. I. Frenkel,[2] J. Hanson,[1] P. Northrup,[1] and W. Ku[1]

[1]*Brookhaven National Laboratory, Upton, New York 11973, USA*

[2]*Yeshiva University, New York, New York 10016, USA*

(Received 23 March 2007; published 18 July 2007)

Significant nanoscale disorder of Cu and Ca atomic substitution is observed in $CaCu_3Ti_4O_{12}$, based on our integrated study using quantitative electron diffraction and extended x-ray absorption fine structure. Unambiguous identification of this previously omitted disorder is made possible by the unique sensitivity of these probes to valence-electron distribution and short-range order. Furthermore, first-principles-based theoretical analysis indicates that the Ca-site Cu atoms possess partially filled degenerate $e_g$ states, suggesting significant boost of dielectric response from additional low-energy *electronic* contributions. Our study points to a new route of enhancing dielectric response in transitional metal oxides by exploiting the strong electronic correlation beyond classical static pictures.

DOI: 10.1103/PhysRevLett.99.037602 PACS numbers: 77.84.−s, 61.14.Lj, 71.20.−b, 78.70.Dm

The recent discovery of the prodigiously high dielectric constant ( $\sim 10^5$) of cubic $CaCu_3Ti_4O_{12}$ (CCTO), the highest ever measured in nonferroelectrics over a wide range of temperature and frequency, attracted much attention [1–11]. Density functional theory (DFT) calculations based on the ideal stoichiometric single crystal suggest that the material can only have an intrinsic dielectric constant four orders of magnitude less than that observed experimentally [7]. After an exhaustive search for its intrinsic mechanism, attention was then shifted to defects that form the ''internal barrier layer capacitance'' (IBLC) responsible for this anomalous behavior. Various morphological models were proposed [8]. The puzzling aspect is that the long-expected twin boundaries in the system acting as the IBLC were never truly observed [10]. Furthermore, the type and density of the defects are very different in single crystals, bulk ceramics, and thin films of CCTO [4], yet all exhibit similar dielectric behavior [10]. Clearly, there is a general interest as well as an urgent need to understand the origin of the unusual dielectric property in CCTO. The understanding can lead the exploration for the next generation of high-dielectric materials.

In this Letter, we report our study of nanoscale disorder in single crystals of CCTO using unique techniques that are sensitive to local structural disorder. We reveal that there is considerable substitutional disorder at the Ca/Cu sites in the system that was not observed by using volume-averaged scattering probes. We demonstrate that the enhanced *electronic* dielectric response in CCTO can be attributed to the change of local electronic structure associated with Cu substitution of Ca.

CCTO has a cubic cell that is $2 \times 2 \times 2$ times the size of the perovskite subcell $ABO_3$, with Ca/Cu at the $A$ sites and Ti at the $B$ sites. Because of the fairly large tilt of the $TiO_6$ octahedra, $\frac{3}{4}$ of the $A$ atoms (i.e., the Cu atoms, hereafter denoted as an $A''$ site with an $mmm$ symmetry) are coordinated with four oxygen atoms forming a square with a Cu atom at the center. The remaining $A$ atoms, Ca ($A'$ site with a $m$-3 symmetry), have a bcc arrangement, and each is surrounded by a 12-oxygen icosahedral environment.

We investigated the same single crystals that were studied previously by neutron scattering and optical conductivity [2]. The recent development of quantitative electron diffraction (QED) [12–14] allows us to determine valence electronic density by accurate measurement of low-order structure factors due to the high sensitivity of small-angle-scattered incident electrons to atomic ionicity and to the distribution of valence electrons that bond atoms together. CCTO has several short scattering vectors because of its relatively large cell dimension; hence, we can take advantage of the QED technique, the paralleling recording of dark-field images (PARODI) method that we developed recently to study valence-electron distribution in crystals with a large unit cell [15,16]. Although PARODI is more technically demanding than conventional convergent beam electron diffraction, it is more suitable to study crystals with a large unit cell using small convergent angles.

The structure factors of low-order reflections were measured using a 300 kV field-emission microscope with a post column energy filter, and compared with first-principles-based DFT calculations. Starting with the structure factors of free atoms, we simulate the diffraction patterns using dynamic diffraction theory and compare them with the experiment via a refinement procedure until a good agreement is reached. These experimental structure factors are model independent. Figures 1(a) and 1(b) are an example of structure factor measurement of CCTO using QED with the comparison of experiment and calculation [Fig. 1(c)]. We concentrate on the six innermost reflections (110, 200, 211, 220, 400, and 422) that are most sensitive to the charge and orbital electrons, but negligibly influenced by the precision of atomic positions and thermal parameters. For reflections further out in reciprocal space, synchrotron x-ray diffraction (XRD) was used. The electron and x-ray data sets were combined, providing experimental measure-

 

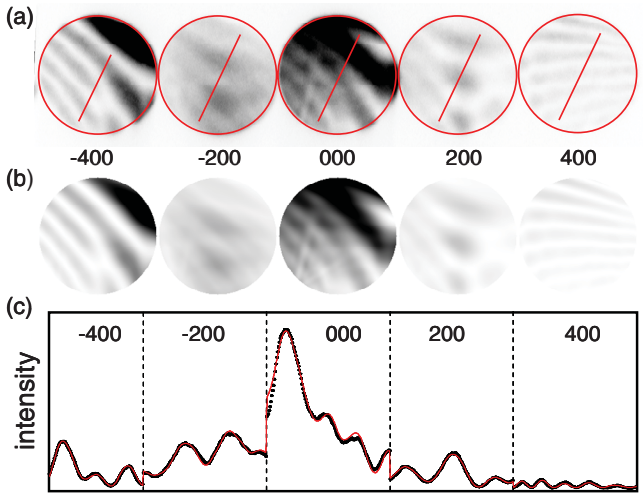


FIG. 1 (color). Measurement of low-order structure factors using quantitative electron diffraction. (a) An experimental PARODI pattern of CCTO recorded on a 20 bit imaging plate showing the h00 systematical row of the 000, ±200, and ±400 reflections at room temperature. (b) Calculated pattern using the dynamic Bloch-wave approach. (c) Line scans of the intensity oscillation from (a) as open circles are compared with calculations in (b) as solid lines. The best fits of the experimental data and calculations yield structure factors of low-order reflections that are the foundation of our bonding-electron measurement, as well as revealing the disordered structure in the system.

ments of 58 independent structure factors, and then converted to x-ray structure factors, which are the Fourier components of charge density. Inverse Fourier transform and multipole refinement [17] of the data yield 3D charge-density distribution.

Figure 2(a) is the resulting experimental density map of CCTO showing bonding valence states in the (001) plane, along with that calculated by DFT [Fig. 2(b)] within the LDA + $U$ approximation. The magnetically active and orbital-ordered Cu-$d$ states exhibit a well-defined $t_{2g}$ symmetry [pointing toward the (110) directions], and form antibonds with neighboring O-$p$ states, in good agreement with calculations. Surprisingly, the states at $A'$ sites that are supposed to be occupied by Ca also show orbital anisotropy with weak $e_g$ symmetry in Fig. 2(a), in clear contrast to the spherical density profile of $Ca^{2+}$ obtained from the theoretical density map [Fig. 2(b)]. Since Cu atoms are the only ones that have open $d$ shell in this system, this immediately points to a considerable amount of Cu substitution of Ca atoms. Similarly, the structure factors determined experimentally at 300 and 90 K are overall in good agreement with DFT calculations, except those of the three innermost reflections that are sensitive to the bonding electrons, which show significant deviation from the calculations. Nevertheless, when $A$-site (Ca and Cu) disorder, as we reported previously [10], was taken into account, the deviation in refinement fell by a factor of 6. This suggests that the stoichiometrically ordered structure of CCTO used in our DFT calculations is inadequate for

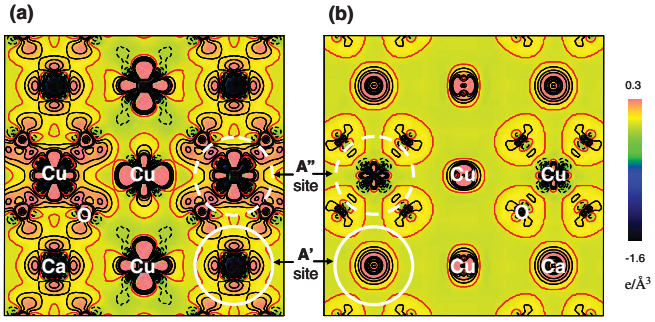


FIG. 2 (color). The bonding-electron distribution of CCTO in (001) basal plane containing Cu, Ca, and O atoms. (a) Experimental observation extracted from structure factor measurements using combined electron and x-ray diffraction data (i.e., the static deformation electron density map using neutral atoms as a reference). (b) DFT calculation based on the ideal crystal structure. The color legend indicates the magnitude of the charge, and the contour plot has an interval of 0.1 e/Å$^3$. The orbital-ordered Cu 3$d$ states of $xy$ symmetry are clearly visible, as well as its antibonding with O 2$p$ states. Note the significant difference near the $A'$ sites (circled by solid line) between (a) and (b), where an anisotropic density pattern of $e_g$ electrons is observed only experimentally, suggesting some degree of disorder with Cu replacing Ca in real material.

describing the electronic structure, particularly, the dielectric response.

To further explore local disorder, we conducted an extended x-ray absorption fine structure (EXAFS) study that is sensitive to local structure around selected atomic species and thus can provide unbiased information about short-range order. The experiments were carried out at NSLS beam lines X11A for Ti and Cu and X15B for Ca, and all edges were analyzed concurrently using the UWXAFS package [18] that allows us to fit theoretically calculated EXAFS signals (using the FEFF6 program [19]) to all three absorbing elements' data. Because of the multiple constraints imposed on the heterometallic bonds during their analysis from either edge, the total number of adjustable variables (18) was much smaller than the number of relevant independent data points (43). Figure 3 shows the experimental EXAFS data, superimposed on their theoretical fits. Among several structural parameters varied in the fits (e.g., metal-oxygen and metal-metal bond lengths and their disorders), the coordination numbers of bonds between $A$-site atoms (Cu, Ca) are particularly important for quantifying the short-range order in this system. Unexpectedly, the Cu-Ca and Ca-Cu coordination numbers $N$ that varied independently in the fits were found to be 3.2 ± 0.8 and 2.4 ± 1.6, respectively, i.e., outside the ranges corresponding to the stoichiometric structure: $1.5 < N_{\text{Cu-Ca}} < 2$ and $4.5 < N_{\text{Ca-Cu}} < 6$. Each result independently points to the presence of a locally Ca-rich phase $CaCu_{1-x}TiO_3$, where $x > 0.25$, suggesting the presence of local compositional disorder. Since XRD shows that the overall sample composition ($x = 0.25$) is preserved, our results unambiguously point to the coexistence of non-

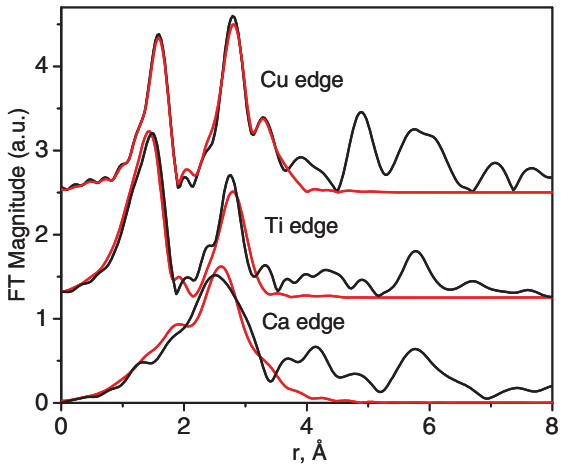


FIG. 3 (color). The Ti, Cu, and Ca $K$ edges of the EXAFS data (black) and their theoretical fits (red). Some data and fits are rescaled and shifted vertically for clarity. The $k$ ranges for Fourier transforms (uncorrected for the photoelectron phase shifts) for Cu, Ti, and Ca were from 2 to 15, 13, or 10 Å$^{-1}$, respectively. The first peak in the Ti EXAFS data is due to the first nearest neighbor Ti-O bonds. The second peak in the Ti data is due to the mixture of Ti-Ca and Ti-Cu contributions. The similar range of distances in Cu is contributed by Cu-O, Cu-Ti, Cu-Ca, and Cu-Cu paths. For better contrast of Cu-Ca and Cu-Cu contributions, we weighted the Cu data with $k^3$ in the analysis, and all others with $k^2$. For Ca atoms, the relatively low value of $k_{\max} = 10$ Å$^{-1}$ does not allow the visual resolution of four contributions (Ca-O, Ca-Ti, Ca-Ca, and Ca-Cu) to the $r$ range between 1 and 4 Å corresponding to the broad first peak in Ca EXAFS. These contributions were accounted for in the data analysis.

stoichiometric nanophases with $x < 0.25$. Presence of local structural disorder is also independently supported by the results of Ti-A and Cu-A bond length measurements that were found to be shorter for $A =$ Ca (3.18 ± 0.02 Å and 3.68 ± 0.02 Å, respectively) than for $A =$ Cu (3.22 ± 0.01 Å and 3.74 ± 0.02 Å, respectively). While such deviations of the local structure inferred from EXAFS from the average structure, ascertained by XRD, may merely indicate local bond buckling of the *actual* structure around the *average* lattice [20] and do not necessarily require local deviations from stoichiometry, the sign of the bond length mismatch is not consistent with a single-phase substitutional alloy since the ionic size of Cu (0.65 Å) is smaller than Ca (0.99 Å). Such difference is expected, however, in a system separated into several, disjoint, off-stoichiometric phases. The fact that the Cu environment is more strongly disordered than that of Ca means that Cu-rich regions have lower dimensionality than the Ca-rich ones.

We note that the local disorder in CCTO measured by EXAFS has not been revealed by previous studies of XRD [3], similar to other analogous systems [21–23]. Observation of local disorder in CCTO is not straightforward because in its $I3m$ structure the substitution of Cu at Ca sites, or vice versa, results in changes only in the intensity of the *ooe* class of reflections ($o$ and $e$ refer to odd and even numbers, respectively) but does not result in any change to the *eee* reflections. Consequently, the normal least squares refinement parameters for the entire data set are not very sensitive to the substitution and the change of the goodness of fit with and without 5% substitution is negligibly small. Nevertheless, our finding agrees with the recent observations, from atomic-pair distribution function analysis, that in CCTO there is unusual temperature dependence of the displacement and significant bonding strain of Ca and Cu under a stoichiometric atomic environment [11]. As discussed above, our multiple-edge study of EXAFS further suggests that the Cu-rich regions are more disordered, or have reduced dimensionality, than the Ca-rich ones. This is consistent with our DFT-based formation-energy calculations that the Ca-rich phase is energetically favorable while the Cu-rich one is not, in agreement with our TEM observations. We found no evidence of enhanced values of Cu-O, Ti-O, or Ca-O bond length disorder (compared to thermal disorder), thus ruling out measurable oxygen-atom disorder and, in turn, its possible role in conductivity. Similar disordered nanoscale phases were previously observed with EXAFS [24,25].

The observed local disorder provides an interesting "extrinsic" feature that may account for the huge dielectric response of CCTO. As illustrated in Fig. 4, analysis of the local symmetry of low-energy electron orbitals shows that while the $t_{2g}$ states of Cu at the ideal $A''$ site support the insulating phase by splitting the degeneracy via orbital ordering (accompanied by tilting of the $TiO_6$ octahedra), the $e_g$ states of Cu located at the Ca site ($A'$-site Cu) remain degenerate within the local cubiclike symmetry, as evident from our DFT calculation. Therefore, in the presence of intersite $d$-$d$ transition or on-site transition permitted by weak (e.g., phonon-assisting) symmetry breaking, a singularly large "metallic" dielectric response is expected near the $A'$-Cu sites. Since the insulating characteristics of the bulk material are only derived from the orbital ordering, significant enhancement of the dielectric response in the nearby *insulating* region can result from various "proximity effects," including their coupling to the $A'$-site-Cu states as well as the disruption of their orbital ordering that leads to low-energy excitons (e.g., reduced local charge gap and the so-called "orbiton" excitations in the gap). In a simplest picture, the local dielectric response would feature singularly large value centered at each $A'$-site Cu with a smooth decay in space. Formulated in a continuous model (with zero-dimension conducting regions), the bulk dielectric function $\varepsilon_{\text{tot}}^{-1} = \frac{1}{V}\int \varepsilon^{-1}(x)d^3x$ could reach very large values, provided that only a very small portion of the volume is far from any of the $A'$-site Cu, as suggested by our EXAFS data, to possess small enough local dielectric response that dominates the integral.

The existence of large volume fraction of high-dielectric *insulating* regions in this picture resolves a dilemma of

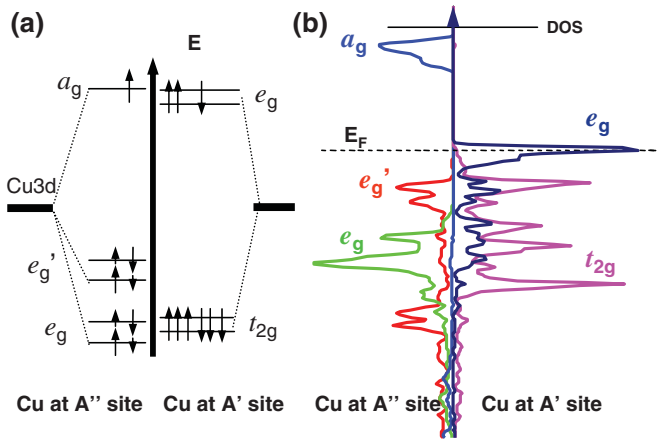


FIG. 4 (color). Tendency towards degeneracy in disordered Cu $3d$ in CCTO ($A'A''_3Ti_4O_{12}$). Left: Cu at $A''$ site ($mmm$) with $A' = $ Ca. Right: Cu substituting at one of the two $A'$ sites ($m$-3) with $A'' = $ Cu in the 40-atom unit cell. (a) Symmetry analysis of degeneracy of local $d$ electronic states of Cu. (b) Partial density of spin-minority states (states per electronvolt cell spin) of Cu based on DFT (LSDA + $U$, $U = 4$ eV) calculations of periodic systems. The Fermi level lies at zero energy. In the ideal CCTO (left), the orbital ordering associated with the $O$-octahedral tilt breaks the degeneracy of $t_{2g}$, while in the disordered region (right) the cubiclike symmetry at the $A'$ site retains the $e_g$ degeneracy, and thus exhibits metalliclike behavior and enables a large local dielectric response.

several proposed conventional extrinsic models [8]; i.e., only a very small fraction ( $\sim 10^{-3}$) of insulating regions is allowed, yet the transport has to be totally impeded without the surface-blocking layers. Furthermore, the crucial role of disorder in our picture provides a natural resolution to the well-known puzzle of why $CdCu_3Ti_4O_{12}$ has a very different dielectric response from that of CCTO despite their almost identical electronic structures and similar sizes of Cd and Ca: the nature of the intrinsic disorder could be very different in the two materials. In fact, our viewpoint on the importance of disorder is indirectly supported by recent experiments [26,27].

In summary, our integrated study using QED, XRD, EXAFS, and first-principles theory evidently reveals the existence of nanoscale disorder of Cu/Ca and suggests its remarkable effects on the dielectric properties of CCTO. Specifically, the higher local symmetry of the $A'$ site recovers the orbital freedom of Cu when substituting Ca, which, in turn, can induce a metalliclike polarizability in the surrounding insulating regions, hence yielding drastically enhanced *dynamical electronic* dielectric response. We propose that such significant enhancement of dielectric response due to disorder-induced recovery of orbital degeneracy is a genuine feature in orbital-ordered strongly correlated electron systems. This microscopic mechanism of boosting the dielectric response opens a door to the design of new functional materials in strongly correlated insulators, such as manganites, by utilizing their orbital freedom via tailoring atomic substitution and disorder.

We thank S. Wakimoto for providing the single crystals and M. H. Cohen, D. Vanderbilt, and J. Tafto for stimulating discussions. Work at Brookhaven was supported by the U.S. Department of Energy, Office of Basic Energy Science, under Contracts No. DE-AC02-98CH10886, No. DE-FG02-05ER36184, and DOE-CMSN.

*Corresponding author.
zhu@bnl.gov

[1] M. A. Subramanian, D. Li, B. A. Reisner, and A. W. Sleight, J. Solid State Chem. **151**, 323 (2000).
[2] C. C. Homes, T. Vogt, S. M. Shapiro, S. Wakimoto, and A. P. Ramirez, Science **293**, 673 (2001).
[3] M. A. Subramanian and A. W. Sleight, Solid State Sci. **4**, 347 (2002).
[4] W. Si *et al.*, Appl. Phys. Lett. **81**, 2056 (2002).
[5] Y. Liu, R. L. Withers, and X. Y. Wei, Phys. Rev. B **72**, 134104 (2005).
[6] D. C. Sinclair, T. B. Adams, F. D. Morrison, and A. R. West, Appl. Phys. Lett. **80**, 2153 (2002).
[7] L. He, J. B. Neaton, M. H. Cohen, D. Vanderbilt, and C. C. Homes, Phys. Rev. B **65**, 214112 (2002).
[8] M. H. Cohen, J. B. Neaton, L. He, and D. Vanderbilt, J. Appl. Phys. **94**, 3299 (2003).
[9] S.-Y. Chung, I.-D. Kim, and S.-J. L. Kang, Nat. Mater. **3**, 774 (2004).
[10] L. Wu *et al.*, Phys. Rev. B **71**, 014118 (2005).
[11] E. S. Bozin *et al.*, J. Phys. Condens. Matter **16**, S5091 (2004).
[12] J. M. Zuo, M. O'Keeffe, and J. C. H. Spence, Nature (London) **401**, 49 (1999).
[13] L. Wu *et al.*, Phys. Rev. B **69**, 064501 (2004).
[14] L. Wu, Y. Zhu, and J. Tafto, Phys. Rev. Lett. **85**, 5126 (2000).
[15] Y. Zhu, L. Wu, and J. Tafto, special issue on Quantitative Electron Diffraction, edited by J. Spence [Microsc. Microanal. **9**, 442 (2003)].
[16] L. Wu, M. A. Schofield, Y. Zhu, and J. Tafto, Ultramicroscopy **98**, 135 (2004).
[17] N. K. Hansen and P. Coppens, Acta Crystallogr. Sect. A **34**, 909 (1978).
[18] E. A. Stern, M. Newville, B. Ravel, Y. Yacoby, and D. Haskel, Physica (Amsterdam) **208&209B**, 117 (1995).
[19] S. I. Zabinsky, J. J. Rehr, A. Ankudinov, R. C. Albers, and M. J. Eller, Phys. Rev. B **52**, 2995 (1995).
[20] A. Frenkel *et al.*, Phys. Rev. Lett. **71**, 3485 (1993); Solid State Commun. **99**, 67 (1996); Phys. Rev. B **62**, 9364 (2000).
[21] D. Haskel *et al.*, Phys. Rev. Lett. **76**, 439 (1996).
[22] N. Sicron *et al.*, Phys. Rev. B **50**, 13 168 (1994).
[23] B. Rechav *et al.*, Phys. Rev. Lett. **72**, 1352 (1994).
[24] E. Prouzet, E. Husson, N. DeMathan, and A. Morell, J. Phys. Condens. Matter **5**, 4889 (1993).
[25] A. I. Frenkel *et al.*, Phys. Rev. Lett. **89**, 285503 (2002).
[26] R. Zuo, L. Feng, Y. Yan, B. Chen, and G. Cao, Solid State Commun. **138**, 91 (2006).
[27] T.-T. Fang, L.-T. Mei, and H.-F. Ho, Acta Mater. **54**, 2867 (2006).